BACKGROUND AEROSOLS AND MULTIPLE FIELD-OF-VIEW LIDAR

Gilles Roy [1], Luc R Bissonnette [1] and Nathalie Roy [2]
[1] Defence Research and Development Canada Valcartier, 2459 Pie XI Blvd. North, Val-Belair (Québec), Canada,
[2] Lidarcam, 110 rue Légaré #26, Loretteville (Québec), Canada, G2B 1X5
gilles.roy@drdc-rddc.gc.ca; luc.bissonnette@drdc-rddc.gc.ca; nathalie.roy.lidarcam@drdc-rddc.gc.ca

ABSTRACT

We investigate the use of multiple scattering via Multiple-Field-Of-View (MFOV) lidar signals to characterize background aerosol particle size and concentration from ground based lidar over distances shorter than a kilometer. The MFOV lidar signal is calculated for background aerosols for a probing wavelength of 266 nm and for visibilities of 5 km and 30 km. The optical depths studied are small and the calculations are restricted to second order scattering. Also since background aerosols are constituted of relatively small particles which diffuse the light at large angles, the chosen full angle fields of view (FOVs) range from 1 to 100 mrad . We show that the MFOV lidar measurements at 266 nm contain exploitable information on particle size and extinction.

1. INTRODUCTION

Atmospheric aerosols play an important role in many atmospheric processes. Ideally we would like to know their basic physical characteristics, i.e., their size, their number and their albedo. Extinction caused by particles smaller than the incident radiation wavelength shows a strong dependence on the wavelength. Several groups using multi-wavelength lidars have exploited this wavelength dependence with success. However, the fundamental problem these methods are facing is that they are limited to submicron particles because particles larger than the probing wavelength do no show appreciable wavelength dependence. Chapter 4 of reference [1] gives a very good review of the state of the art work done in that field. Atmospheric aerosols are usually multimodal; their particle size density distribution is very often represented by a bimodal log-normal distribution and the second mode of this distribution, composed mainly of large particles, is often dominant, as far as optical transmission is concerned. We propose to join to multiple wavelength measurements and MFOV measurement. This measurement could be done with a gated intensified CCD camera as in [2]. In this paper we present the second order scattering model used to generate MFOV lidar signals for various atmospheric aerosol size density distributions. MFOV lidar returns are calculated for the Nd-YAG fourth harmonic wavelength (266 nm). A modified version of the MFOV lidar data inversion algorithm developed for clouds [3] is applied to the synthetic lidar return to retrieve the effective diameter of background aerosols as well as the extinction. Two aerosol size density distributions, 2 visibilities (5 km and 30 km) and 2 penetration depths (400 m and 800 m), for a total of 8 MFOV lidar signals have been simulated. A comparison of the retrieved parameters with the true parameters provides a quantitative evaluation of the proposed method.

2. SCATTERING MODEL

Atmospheric aerosols

The aerosol number density distribution is represented by the following bimodal log-normal distribution

$$\frac{dN(r)}{dr} = \sum_{i=1}^{2}\left(\frac{N_i}{\ln(10) * r * s_i * \sqrt{2\pi}}\right)\exp\left[-\frac{(\log r - \log r_i)^2}{2\, s_i^{\,2}}\right] \tag{1}$$

where $N(r)$ = number density distribution of radius r,
s_i = the geometric standard deviation for the mode i,
N_i = the relative number of particles for the mode i,
r_i = mean radius for the mode i.

Two density distributions are considered. Their input parameters are listed in Table I. The distributions have been truncated at 100 µm. The complex refractive index is set to 1.36-i0.00457 for both distributions.

Table I : Aerosol number density distribution parameters

	Distribution Type I	Distribution Type II
r_1 (µm)	0.05	0.15
r_2 (µm)	1.0	3
s_1	0.35	0.35
s_2	0.4	0.4
n_1	0.999875	0.99
n_2	0.000125	0.01

Rayleigh and aerosol scattering

At 266 nm, it is necessary to take molecular Rayleigh scattering into account when performing calculations. So, the following "definitions" have been used in our model:

$\alpha = \alpha_a + \alpha_R$; where α_a : the aerosol extinction; α_R : Rayleigh extinction;

$\alpha_{a,s} = \varpi_0 \alpha_a$; $\alpha_{a,s}$: the extinction caused by scattering; ω_0 is the albedo;

the effective phase function is expressed by:

$p(\beta) = (\alpha_{a,s} p_a(\beta) + \alpha_R p_R(\beta)) / (\alpha_{a,s} + \alpha_R)$;

$p_a(\beta)$ is the aerosol phase function obtained from application of Mie calculations to the particle size density distribution of interest

$p_R(\beta) = \frac{3}{16\pi}(1 + \cos^2\beta)$ is the Rayleigh phase function;

$\alpha_R = 1.33x10^{-5}\left(\lambda/0.532\right)^{-4}$ is the Rayleigh extinction.

We want to relate the extinction at 266 nm to the visibility range. The visibility (vis) is defined at 532 nm for a contrast of 2% :

$$vis(meter) = -\ln(0.02)/\alpha(\lambda = 532nm) \qquad (2a)$$

The extinction cross sections (α_{eff}) are calculated for a given aerosol size distribution at the wavelength of interest and at 532 nm, then the ratio of these calculated values is multiplied by the extinction previously obtained from the visibility equation 2a

$$\alpha(\lambda) = \frac{\alpha_{eff}(\lambda)}{\alpha_{eff}(\lambda = 532nm)}\alpha(\lambda = 532nm) \qquad (2b)$$

Table II provides the aerosol extinctions at 532 nm as defined by Eq. 2a and at 266 nm calculated from Eq. 2b for visibilities of 5 and 30 km for the two particle size distributions studied.

Table II: Aerosol extinction coefficients

Visibility (km)	Extinction (1/m)	Extintion (1/m)	
	532 nm	266 nm	
		Type I	Type II
5	7.90E-04	1.26E-03	7.82E-04
30	1.31E-04	2.10E-04	1.30E-04

Single scattering lidar return

For the single scattering, we have the well-known single-scattering lidar equation :

$$P(z_c) = P_0 e^{-2\alpha z_c} \frac{A}{z_c^2}\frac{c\tau}{2}(\alpha\omega_0 + \alpha_R)p(\pi) . \qquad (3)$$

For a laser beam with a divergence of 0.3 mrad, almost all the single scattering is contained in a FOV of 1mrad. Following the usual notation convention for lidar, c , τ and A represent respectively the speed of light, the pulse width and the area of the collecting aperture.

Double scattering

The essence of the multiple field of view lidar technique is the measurement of the scattered power $S(\theta)$ as a function of the receiver field of view θ. The scattered power $S(\theta)$ contains information on scatters size. In Figure 1, the angle θ corresponds to one half of the lidar total FOV. We consider that the laser beam divergence is small and that the scattered power originating from single scattering events is concentrated inside the smallest field of view θ_{min} of the detector. We also assume that the extinction and the particle size of the atmospheric aerosols are spatially homogeneous, and that the time delay of the scattered photons is negligible. According to the previous assumptions, for angles $\theta > \theta_{min}$ the scattered radiation must come from multiple scattering events. The scattered power in the FOV interval $\Delta\theta_i = \theta_{i+1} - \theta_i$ can be calculated using [1]:

$$S(z_c, \Delta\theta_i) = S_0 e^{-2\alpha(z_c - z_a)} \frac{c\tau}{2}\frac{A}{z_c^2} 2\int_{z_a}^{z_c}\int_0^{2\pi}\int_{\beta_j}^{\beta_{j+1}}[\alpha(z)p(r,\beta)] \bullet$$
$$[\alpha(z_c)p(r,\beta_{back})]\sin\beta d\beta d\phi dz \qquad (4)$$

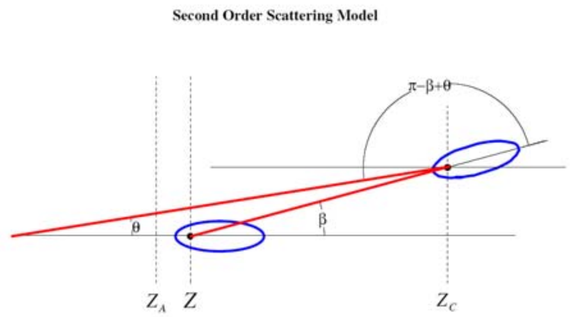

Fig. 1 : Second order scattering detected at an angle θ by the MFOV lidar; the ellipses represent the phase function

The factor 2 in front of the integral is coming from the reciprocity theorem [4], α is the extinction coefficient, $p(r,\beta)$ and $p\ (r,\beta_{back})$ are the values of the phase function for the forward (β), and backward scattering angles ($\beta_{back} = \pi - \beta + \theta$) for a particle of radius r, z_a is the distance to the boundary of the probed aerosol layer, z_c is the range, the quantity $[\alpha(z)p(r,\beta)]$ represents the forward scattering coefficient while $[\alpha(z_c)p(r,\beta_{back})]$ represents the backscattering coefficient, and ϕ is the azimuthal angle ranging from 0 to 2π . From Figure 1, the scattering angle β can be easily related to the FOV θ via the relation $\tan\beta = \dfrac{z_c \tan\theta}{z_c - z}$.

3.0 RESULTS

Figure 2 shows the normalized lidar returns as a function of the FOV for the distributions of Type I and II. We will apply a slightly modified version of our MFOV extinction coefficient and effective diameter recovering algorithm to the 8 MFOV cases studied. For a complete description of the algorithm, consult references [3]; we give here only a summary description. For a homogeneous medium, the effective diameter d_e ($d_e=2\langle r^3\rangle / \langle r^2\rangle$) of particles larger than the wavelength is given by:

$$d_{e2} \cong \kappa \frac{\lambda}{\theta_{md}} \qquad (5)$$

where the subscript 2 refers to the second mode (the large particles), λ is the wavelength, θ_{md} is the angular scale of the FOV dependence of the forward contribution of diffraction scattering to the lidar return (to be determined) and κ is a numerical constant. According to Eloranta double scattering formulation [1,5], a good estimate of the optical depth can be obtained using:

$$\tau_2(z) \cong \ln\left(1 + \frac{\beta_{bs}}{\overline{\beta}_{bs}} \frac{P_{d2}(z,\infty) - P_{d2}(z,\theta_{\min})}{P_{d2}(z,\theta_{\min})}\right) \qquad (6)$$

where $P_{d2}(z,\theta_{\min})$ is the diffraction contribution of the second mode to the lidar return, β_{bs} is the backscattering coefficient including Rayleigh scattering and Mie scattering for the two modes, $\overline{\beta}_{bs}$ is the mean value of β_{bs} calculated over the backscattering angles contributing to $P_{d2}(z,\theta)$, $\theta_{\min}$ is the FOV that contains 99% of the laser beam encircled energy and finally $P_{d2}(z,\infty)$ is the asymptotic value of $P_{d2}(z,\theta)$.
Simulations have shown that the MFOV lidar signals generated for cases where the two atmospheric aerosol modes both contribute significantly exhibit two scales in θ. This condition is verified for the distributions studied here since the relative contribution of each mode depends on the effective diameter as well as the relative number of particles for each mode. Figure 2 illustrates two lidar signals and their two-angular-scale fitted curves given by Eq.7:

$$\frac{P(z,\theta)}{P(z,\theta_{\min})} = A_0(z) + A_1(z) erf(\theta/\theta_1(z)) + A_2(z) erf(\theta/\theta_2(z)) \qquad (7)$$

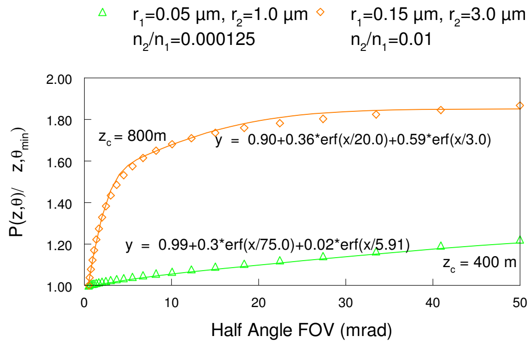

Fig. 2: Lidar return as a function of the FOV, at a probing wavelength of 266 nm, for two aerosol size density distributions for a visibility of 5 km, and for probing distances of 400m and 800m.

where *erf* is the error function and A_0, A_1, A_2, θ_1 and θ_2 are the fitting parameters. Now we assume that the expression $A_2(z) erf(\theta/\theta_2(z))$ in Eq.7 depends mainly of diffraction scattering caused by the large particles of the second mode. The fact that diffraction scattering by the large particles from mode 2 is concentrated into the small FOVs in comparison with the geometric scattering of mode 2 and the global scattering of mode 1 supports this interpretation. This interpretation is applicable to retrieval if the diffraction contribution is indeed significant, which we should be able to quantify with the ratio of A_2 / A_1, i.e., if $A_2 / A_1 > Threshold$ the hypothesis is valid and we can write:

$$A_2(z) \cong \frac{P_{d2}(z,\infty) - P_{d2}(z,\theta_{\min})}{P_{d2}(z,\theta_{\min})} \qquad (8)$$

$$\theta_2(z) = \theta_{md}(z) \qquad (9)$$

where the *Threshold* will be determined from numerical simulations. From parameter A_2 and using Eq. 6 and Eq. 8 we have:

$$\tau_2(z) \cong \ln\left(1 + \frac{\beta}{\overline{\beta}} A_2(z)\right) \qquad (10)$$

The ratio $\beta_{bs} / \overline{\beta}_{bs}$ is unknown a priori, but a value of 1.4 is quite acceptable for many practical cases. Although, it is not completely justified, we will apply here the same model for the calculation of the effective diameter d_{e1} of the first mode. According to these assumptions, the total optical depth could be expressed by :

$$\tau\ (z) \cong \ln\left(1 + \frac{\beta}{\overline{\beta}}[A_1(z) + A_2(z)]\right) \qquad (11)$$

These calculations will allow us to determine the limits of the method.

Table IIIa lists the values of the retrieved effective diameters of mode 1 and 2 (d_{e1} and d_{e2}) while the Table IIIb lists the values of τ. These values have been calculated for the bimodal log-normal distributions listed in Table II. The proportionality constant in Eq. 4 has been set to 0.46 as for water clouds [3]. For the first case, high visibility and short range, the best fit (Eq. 7) failed. For the 7 others cases, good consistency is obtained for the effective diameters especially for the lower visibility and the mode 2 made of larger particle. The recovered effective diameters of mode 1 made up of small particles are systematically 2 to 3 times larger than the true effective diameter. This is certainly related to the fact that the Eq. 5 is no longer valid in this region; but we nevertheless present the results because the error is systematic and some exploitation of the data may still be possible. The estimation of the optical depth shows a higher error but the retrieve values are generally consistent.

Table IIIa : Comparison of the true and recovered effective diameter values

Aerosol	Type I				
Visibility	z_c	d_1(0.5µm)	d_2(16.4µm)	$\Delta d_1/d_1$	$\Delta d_2/d_2$
30 km	400	ind	ind	ind	ind
30 km	800	1.61 µm	31.3 µm	222%	190%
5 km	400	1.58 µm	20.6 µm	216%	26%
5 km	800	1.55 µm	19.4 µm	210%	18%
Aerosol	TypeII				
Visibility	z_c	d_1(1.5µm)	d_2(43.6µm)	$\Delta d_1/d_1$	$\Delta d_2/d_2$
30 km	400	4.94 µm	42.8 µm	229%	-2%
30 km	800	4.64 µm	40.2 µm	209%	-8%
5 km	400	5.8 µm	41.0 µm	287%	-6%
5 km	800	5.96 µm	40.7 µm	297%	-7%

Table IIIb : Comparison of the true and recovered optical depth values

Aerosol	Type I			
Visibility	z_c	τ	τ (eq.#11)	$\Delta\tau/\tau$
30 km	400	0.084	ind	ind
30 km	800	0.168	0.15	-11%
5 km	400	0.5	0.37	-26%
5 km	800	1	0.65	-35%
Aerosol	Type II			
Visibility	z_c	τ	τ (eq.#11)	$\Delta\tau/\tau$
30 km	400	0.052	0.09	73%
30 km	800	0.104	0.17	70%
5 km	400	0.31	0.5	61%
5 km	800	0.62	0.8	29%

4. DISCUSSION AND CONCLUSION

We have shown that in theory the MFOV technique allows the determination of the extinction coefficient and the effective diameters with acceptable precission for particles large compared with the wavelength. The values retrieved could be used as constraints in the multi-wavelength inversion algorithm and consequently a better regularization could be obtained when large particle contribute. Under some conditions, it is also possible to obtain information on the first mode of the distribution.

Work needs to be done to clarify the proportionality constant between the angular scale θ_{md} and the effective diameter. For example, we should explain why the proportionality constant in Eq. 5 appears different for the two modes of the aerosol distribution.

We are now developing a prototype using a UV laser at 266 nm and an intensified CCD camera to validate the concepts developed in this paper and to define its limitations. It's important to note that for short wavelengths the backscattering is significantly higher than for larger wavelengths because the Rayleigh scattering contributions are more important. For the measurement of the second order scattering this is a definite advantage. Also, because the proposed technique involves measuring the small lidar signals in large FOVs, operation in the solar blind region is highly desirable for daylight operation to minimize the background radiation incident on the detector.

REFERENCE

1. Editor Claus Weikamp., *Lidar : Range-Resolved Optical Remote Sensing of the Atmosphere*, (Springer Series in Optical Sciences) (Hardcover), 2005, 455 pp, ISBN 0-387-40075.
2. N. Roy, G. Roy, L. R. Bissonnette, and J.-R. Simard, "Measurement of the azimuthal dependence of cross-polarized lidar returns and its relation to optical depth," *Appl. Opt*. **43,** 2777–2785 (2004).
3. L. R. Bissonnette, G. Roy and N. Roy, "Multiple-scattering-based lidar retrieval: method and results of cloud probings, *Appl. Opt*. **44**, pp.5565-5581 (2005).
4. L. Katsev, E. P. Zege, A. S. Prikhach, and I. N. Polonsky, "Efficient technique to determine backscattered light power for various atmospheric and oceanic sounding and imaging systems," *J. Opt. Soc. Am*. A **14,** 1338–1346 (1997).
5. E.W. Eloranta, "Practical model for the calculation of multiple scattered lidars returns", *Appl. Opt.* **37**, pp.2464-2472 (1998).